Evidence for Gamow-Teller Decay of ^{78}Ni Core from Beta-Delayed Neutron Emission Studies

M. Madurga,[1,2] S. V. Paulauskas,[1] R. Grzywacz,[1,3] D. Miller,[1] D. W. Bardayan,[3] J. C. Batchelder,[4] N. T. Brewer,[3] J. A. Cizewski,[5] A. Fijałkowska,[6] C. J. Gross,[3] M. E. Howard,[5] S. V. Ilyushkin,[7] B. Manning,[5] M. Matoš,[8] A. J. Mendez II,[3,9] K. Miernik,[3,6] S. W. Padgett,[1] W. A. Peters,[10] B. C. Rasco,[8] A. Ratkiewicz,[5] K. P. Rykaczewski,[3] D. W. Stracener,[3] E. H. Wang,[11] M. Wolińska-Cichocka,[12,3] and E. F. Zganjar[8]

[1]*Department of Physics and Astronomy, University of Tennessee, Knoxville, Tennessee 37996, USA*
[2]*ISOLDE, EP Department, CERN, CH-1211 Geneva, Switzerland*
[3]*Physics Division, Oak Ridge National Laboratory, Oak Ridge, Tennessee 37830, USA*
[4]*Department of Nuclear Engineering, University of California, Berkeley, Berkeley, California 94702, USA*
[5]*Department of Physics and Astronomy, Rutgers University, New Brunswick, New Jersey 08903, USA*
[6]*Faculty of Physics, University of Warsaw, Warszawa PL 00-681, Poland*
[7]*Department of Physics, Colorado School of Mines, Golden, Colorado 80401, USA*
[8]*Department of Physics and Astronomy, Louisiana State University, Baton Rouge, Louisiana 70803, USA*
[9]*Department of Physics and Astronomy, Austin Peay State University, Clarksville, Tennessee 37044, USA*
[10]*Oak Ridge Associated Universities, Oak Ridge, Tennessee 37831, USA*
[11]*Department of Physics and Astronomy, Vanderbilt University, Nashville, Tennessee 37235, USA*
[12]*Heavy Ion Laboratory, University of Warsaw, Warsaw PL 02-093, Poland*

(Received 20 April 2016; published 23 August 2016)

The β-delayed neutron emission of ^{83,84}Ga isotopes was studied using the neutron time-of-flight technique. The measured neutron energy spectra showed emission from states at excitation energies high above the neutron separation energy and previously not observed in the β decay of midmass nuclei. The large decay strength deduced from the observed intense neutron emission is a signature of Gamow-Teller transformation. This observation was interpreted as evidence for allowed β decay to ^{78}Ni core-excited states in ^{83,84}Ge favored by shell effects. We developed shell model calculations in the proton $fpg_{9/2}$ and neutron extended $fpg_{9/2}+d_{5/2}$ valence space using realistic interactions that were used to understand measured β-decay lifetimes. We conclude that enhanced, concentrated β-decay strength for neutron-unbound states may be common for very neutron-rich nuclei. This leads to intense β-delayed high-energy neutron and strong multineutron emission probabilities that in turn affect astrophysical nucleosynthesis models.

DOI: 10.1103/PhysRevLett.117.092502

β-delayed neutron emission from fission fragments was first observed in 1939 following the neutron bombardment of uranium salts [1]. It was recognized that the delayed neutron energies and emission probabilities, P_n, are important parameters to model environments that involve neutron-rich isotopes. Two of the main applications are in nuclear reactor physics [2] and r-process nucleosynthesis [3]. Because β-delayed neutron precursors are neutron rich and far from stability, they are always relatively difficult to produce and study. Advances in detector capabilities allowed for pioneering measurements of neutron emission spectra of fission fragments [4,5]. In these experiments, resonancelike behavior was observed in the neutron emission spectrum [4,6].

These efforts were halted in the following decade by several factors. First, it became increasingly difficult to produce species with larger neutron excess. Second, the very influential work by Hardy, Johnson, and Hansen on "pandemonium" attributed the features of the neutron spectra to purely statistical effects and warned against overinterpretation of the measurements [7]. Misinterpretations of their work attributed decay observables of all heavy nuclei to gross features of the decay strength and statistical fluctuations of the level density. A more accurate depiction of their work is that neutron emission characteristics cannot be interpreted without considering the effects of high level density. The pandemonium controversy [8] arose partly from the fact that, at the time, there was no capability to compute nuclear properties using a sufficiently complete microscopic model of the nucleus.

State-of-the-art models are now capable of computing decay properties of atomic nuclei, such as lifetimes and branching ratios. It has become increasingly clear that the β-decay observables are profoundly influenced by nuclear

structure [9–13]. This relationship is particularly strong for nuclei close to shell closures. In abandoning a purely statistical treatment, it is increasingly difficult to reliably predict decay half-lives of neutron-rich nuclei using models tailored to reproduce the structure of species close to stability. Needing to go beyond a statistical treatment also impacts calculations of astrophysical r-process abundances [3,10,14]. The r process [15] involves many neutron-rich nuclei that are difficult or impossible to study experimentally. Network calculations currently depend on predictions made using global models [10,16]. These models continuously evolve and absorb more details of nuclear structure to improve their predictions [12,17].

The β-decay half-life depends on the decay energetics, the masses, and the microscopic structure of the mother and daughter nuclei. The former sets the size of the electron-neutrino phase space, while the latter is captured in the so-called "strength function" [18]. The best test of the accuracy of a model is comparing the calculated strength distribution with that determined from direct observations. Unfortunately, measuring the strength over the entire decay window is a difficult experimental challenge. For neutron-rich nuclei with an increasing number of neutrons, the decay energies increment rapidly while the neutron separation energies decrease. As a result a significant portion of the decay populates neutron-unbound states. Detailed neutron spectroscopy is needed together with traditional gamma spectroscopy in order to measure the complete decay distribution.

In this Letter we present the first measurement of the ^{83,84}Ga β-delayed neutron energy spectrum. Gallium isotopes with $N > 50$ are good candidates to study delayed neutron emission owing to their large decay energy windows, 11.7 and 13.8(4) MeV, respectively [19], and substantial branching ratios, 62.8(25)% and 74(14)% [20,21]. We deduce their β-strength function up to 6 MeV above the neutron separation energies. The key result presented here is the observation of neutrons emitted with energies exceeding 2 MeV. This phenomenon cannot be explained without invoking nuclear shell properties. Because of the proximity of doubly magic ^{78}Ni the valence space is small and the shell model should indeed be used to describe the structure of ^{83,84}Ga. We introduce a new shell model calculation that reproduces the observed intensities by including excitations across the $N = 50$ shell gap in the germanium daughters. This model is used to calculate the decay properties for the $N > 50$ gallium and nickel isotopic chains.

The ^{83,84}Ga isotopes were produced at the Holifield Radioactive Ion Beam Facility (HRIBF) at Oak Ridge National Laboratory using the isotope separation online technique [22]. The 50 MeV proton beam of 10–18 μA intensity induced fission in a UC_x target (4.2 g/cm^2) located at the ion source assembly at the HRIBF high-voltage platform IRIS-2. Radioactive fission products were ionized and selected using a two-stage mass separation. An electrostatic kicker was used to periodically deflect the ion beam after the second-stage separator. The separated ions were transmitted to the Low Energy Radioactive Ion Beam Spectroscopy Station for decay measurements. The 200-keV ions were implanted into a tape in the Moving Tape Collector (MTC) in the middle of the β-γ-neutron counting setup. The MTC was operated in the takeaway mode with 1-second grow-in, followed by 1-second decay cycle, during which the ion beam was deflected away by the electrostatic kicker. The MTC transported the collected samples 50 cm away from the shielded measuring station within 400 ms. The γ radiations were measured using two high-purity Ge (HPGe) clover detectors from the CLARION array [23]. The clover detectors' photopeak efficiency was 31% at 88 keV and 4% at 1.33 MeV. The total number of ^{83,84}Ga decays recorded in our experiment was estimated from the absolute intensity of the 1348.2 and 247 keV lines, respectively [21]. The neutron energies were measured with the newly commissioned TOF instrument, the Versatile Array of Neutron Detectors at Low Energy (VANDLE) [24]. The configuration used here consisted of 48 $3 \times 3 \times 60$ cm^3 plastic scintillator modules capped by photomultiplier tubes at both ends. The VANDLE modules were arranged in two arcs of 24 modules of 50-cm radius each, located above and below the implantation spot. The total angular acceptance of the array was 27.5% of 4π and had an intrinsic neutron detection efficiency of 40% at 1 MeV. The close geometry of the clover detectors caused shadowing of the neutron path in some of the VANDLE modules. Because of shadowing, we focused the analysis of neutron singles in a subset of 10 modules. This reduced the angular acceptance to 5.7% of 4π, and the total efficiency to 2.3% at 1 MeV. Data from the full neutron array were used in coincidence with the HPGe clovers for increased efficiency. Two plastic scintillators surrounding the implantation point detected the beta particles, providing a start signal for VANDLE. Data were taken in β-neutron coincidence mode, requiring both photomultipliers of a detector module and one of the beta triggers to record the event [25]. This triggering method allowed for the rejection of dark-current induced events and lowered the acquisition threshold to approximately 8 keV for photons, resulting in a 70-keV energy threshold for neutrons. The time resolution of the combined beta triggers plus neutron detector modules was estimated from the width of the TOF gamma flash to be 3 ns. VANDLE modules were independently measured to have a time resolution of 700 ps, indicating that the observed poorer timing arises from the performance of the beta trigger. More details of the analysis will be presented in a future publication [26].

Neutron time-of-flight spectra for ^{83,84}Ga, from the unobstructed subset of VANDLE modules, are shown in the left column of Fig. 1, panels (a) and (b). A peak in ^{84}Ga at 25 ns containing 50% of the intensity stands out clearly

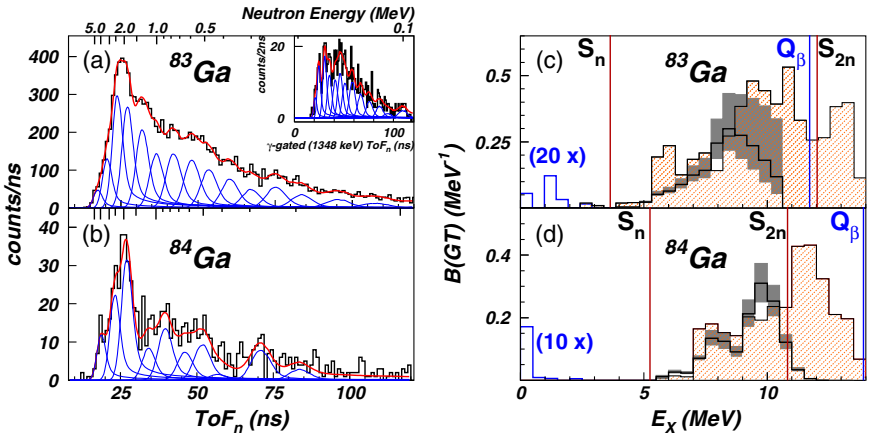

FIG. 1. Left: β-delayed ^{83}Ga (a) and ^{84}Ga (b) neutron time-of-flight (TOF) spectra. The minimum χ^2 fit (red line) was obtained using 16 (^{83}Ga) and 10 (^{84}Ga) neutron quasiresonances, in blue (see the text for more details). The inset shows the neutron time-of-flight spectrum in coincidence with the 1348 keV line in ^{82}Ge. Right: Gamow-Teller (GT) strength distribution above the neutron separation energy in the decay of ^{83}Ga (c) and ^{84}Ga (d). The data are shown in a solid black line and the grey shaded parts of the histogram indicate the uncertainties of the strength distribution. The strength distributions extracted from β-delayed gamma-ray spectroscopy are shown by blue lines, enhanced by factors of 20 and 10 for ^{83}Ga and ^{84}Ga, respectively [29,30]. The dashed histogram shows the Gamow-Teller strength from our shell model calculation using the ^{56}Ni core.

from the rest of the spectrum. Because of the limited resolution of the TOF technique this peak does not reflect a single large resonance. Instead, it indicates that a large fraction of the neutrons is emitted with energies above 1.5 MeV. Such large energy neutron emission observed in both gallium isotopes is unusual for midmass nuclei. Previous experiments in the region [6,27,28] observed very low intensity above 1 MeV and negligible emission above 2 MeV. The origin of the high-energy neutron emission is discussed below.

The goal of our analysis of the neutron TOF data was to obtain the neutron distribution as a function of energy. In classical studies of β-delayed neutron emission in light nuclei individual neutron-emitting states can be observed (see, e.g., [31,32]). As indicated in the introduction, the neutron energy distribution of midmass nuclei studied using limited resolution devices does not correspond to individual resonances [7]. It is determined by the β-decay feedings, level density, and final states in the $N-1$ daughter. Considering the delayed neutron emission is observed as a continuum of lines in our experiment, we performed the analysis accordingly. First, the full response function of our detector system to monoenergetic neutrons was simulated with GEANT4 and convoluted with the experimental time resolution described above. Then, these response functions were utilized to fit the TOF spectrum, using the minimum possible number of them to achieve χ^2/d.o.f.. close to 1 [blue lines in panels (a) and (b) of Fig. 1]. This method allowed us to describe fully the experimental neutron TOF [red line in panels (a) and (b) of Fig. 1]. To calculate the β-decay feedings (I_β) and Gamow-Teller decay strength [B(GT)], the fit was interpreted as describing a continuous distribution. Each fit peak corresponded to a distribution of unresolved neutron lines with its width determined by the TOF resolution. We calculated I_β by normalizing the neutron intensity distribution to the total number of decays observed during the experiment. The same fitting method was used with the neutron spectra in coincidence with the ^{82}Ge gamma lines at 415.7, 596.4, 727.6, 867.2, 938.8, 985.1, 1176.1, 1348.2 (see the inset in Fig. 1), 1354.0, and 1365.4 keV and the ^{83}Ge 247 keV line [21]. The feeding to excited states in the N-1 daughter extracted from the coincidences was then used to correct the I_β distribution. Finally, the GT decay strength as a function of the excitation energy was derived from the I_β [18]; see Fig. 1 panels (c) and (d). The resulting strength inside the experimental energy window corresponds to summed B(GT) of 2.0(4) and 1.4(3) MeV^{-1} for ^{83,84}Ga, respectively.

We determined the neutron branching ratios (P_n) from the resulting fit amplitudes, obtaining 56(7)% for ^{83}Ga and 40(7)% for ^{84}Ga. The literature value for ^{83}Ga, 62.8(25)% [20], compares well with our result. On the other hand, the branching ratio of 74(14)% reported by Winger *et al.* for ^{84}Ga [21] is larger than our value. This difference could be explained if a substantial portion of the delayed neutrons are emitted at energies below our 70-keV threshold. However, recent independent measurements of the ^{84}Ga neutron branching ratio point to a smaller value of P_n, 20 (20)% [33] and 51(28)% [34], respectively. One possible origin of the discrepancy with the work by Winger *et al.* may be the uncertainty in extracting the ^{84}Ga partial branching ratio of neutrons decaying to the ground state of ^{83}Ge using ^{83}Ge β-decay gamma lines [21]. This hypothesis is supported by a good match between the

reported 7.9(9)% neutron feeding to the 247 keV state [21] and our result of 11(3)%.

The experimental strength distribution extracted from the fit is shown in the right column of Fig. 1, panels (c) and (d). A binning of 0.5 MeV was chosen to correspond to the time-of-flight resolution of the 50-cm flight path. The experimental error bars represent the combined statistical and systematic uncertainty. The systematic error arises from the variation of the Fermi phase-space factor f over the 0.5-MeV binning interval. This effect is responsible for the large uncertainty in ^{83}Ga at energies close to the Q_β value. In both gallium isotopes, the most distinct features are an apparent threshold effect, and fluctuations forming visible steps in the ^{84}Ga $B(\mathrm{GT})$. Interestingly the strength begins to increase at about 6–7 MeV and reaches large values up to 0.3 MeV^{-1}. Such large values clearly indicate that the decay above the neutron separation energy is dominated by allowed Gamow-Teller transitions.

To explore the connection between the observed data and the nuclear structure, we did shell model calculations employing the NuShellX code [35] with realistic interactions and built-in GT operators. Our first calculations were performed within the configuration space including proton orbitals $f_{5/2}$, $p_{1/2}$, $p_{3/2}$, and $g_{9/2}$ and neutron orbitals $s_{1/2}$, $d_{5/2}$, $g_{7/2}$, and $h_{11/2}$ with a ^{78}Ni core and the $jj45pna$ [36] set of matrix elements. Our model predicts $5/2^-$ spin parity for the ^{83}Ga ground state, similar to the previously observed ground state of ^{81}Ga [37]. In the case of ^{84}Ga our calculations predict quasidegenerate 2^- and 3^- states. We used the ground state configuration corresponding to the 2^- state following the observation of the same ground state spin parity in ^{82}Ga [29,38]. For both ^{83,84}Ga the resulting calculated β-strength distributions were 2 orders of magnitude smaller than large strength observed in the experimentally accessible region. This observation was perhaps not very surprising because within the chosen configuration space only the single orbitals $\pi g_{9/2}$ and $\nu g_{7/2}$ could contribute to allowed transitions. We found that for the $N = 52$, 53 gallium isotopes the $\nu g_{7/2}$ orbital contributes very little to the ground state wave functions.

We then extended the neutron valence space to the spin-orbit partners of the pfg proton orbitals. Here we used an inert ^{56}Ni core with realistic $jj44bpn$ interactions [37]. This configuration space corresponds to the $f_{5/2}$, $p_{1/2}$, $p_{3/2}$, and $g_{9/2}$ orbitals for protons and neutrons plus the $d_{5/2}$ neutron orbital (see Fig. 2). For tractability, neutron orbitals above the $d_{5/2}$ were excluded, following current experimental evidence for ground states in the region [39,40]. This allowed for much faster calculations while preserving spin-parity rules in both parent and daughter nuclei. Again, we obtained a $5/2^-$ ground state of ^{83}Ga and used the 2^- state for ^{84}Ga. The single particle energies were chosen based on the empirical analysis by Grawe [41]. The $N = 50$ shell gap between $\nu d_{5/2}$ and $\nu g_{9/2}$ orbitals was set to

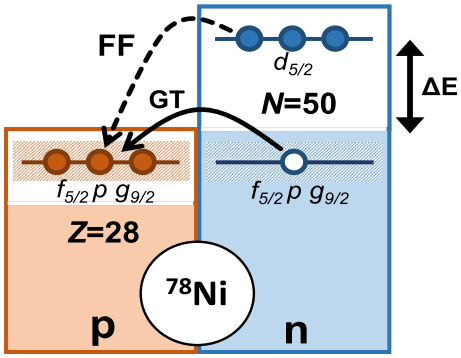

FIG. 2. Schematic of β decay of ^{84}Ga into ^{84}Ge. The GT decay proceeds via transformation of neutrons in the ^{78}Ni core orbitals ($f_{5/2}$, $p_{3/2}$, $p_{1/2}$, and $g_{9/2}$) into protons occupying their spin-orbit partners outside the $Z = 28$ core. These transitions are coupled with very strong matrix elements. The alternative decay mode, through the first forbidden (FF) $d_{5/2} \rightarrow f_{5/2}$ transformation, populates neutron bound states in ^{84}Ge.

3.9 MeV as predicted by Moller *et al.* [42]. It was necessary to construct a new set of residual interactions enabling the couplings between $\nu d_{5/2}$ and fpg-shell protons and neutrons. An additional set of matrix elements was added to build the new hybrid interactions in a schematic way, utilizing interactions for the $f_{5/2}$ orbital. Our hybrid interaction has also been tested to interpret the β-decay gamma spectroscopy from decays of other $N > 50$ nuclei [29,43].

The right column of Fig. 1 shows the experimental $B(\mathrm{GT})$ values for ^{83,84}Ga, panels (c) and (d), respectively, superimposed with our $B(\mathrm{GT})$ calculations. We incorporated a quenching factor of 0.5 in the theoretical strength of both ^{83,84}Ga. The quenching is necessary due to the incomplete neutron configuration space in our model affecting the normalization of the wave functions after diagonalization [44]. For completeness, we included the strength feeding neutron bound states, taken from [29,30]. These matrix elements to bound states are 1 order of magnitude smaller and therefore likely to be forbidden transitions and are not included in our calculations. We obtain good agreement between the experimental $B(\mathrm{GT})$ distributions and our model. The total amount of strength, its location above the neutron separation energy, and the steplike fluctuation in the strength are all well reproduced. These fluctuations arise in our model from the changes in the density of GT allowed states in ^{83,84}Ge. The first substantial increment of the decay strength, at around the neutron separation energy, is associated with opening the $\nu f_{5/2}$ orbital. It must be noted that the large increase in $B(\mathrm{GT})$ with energy naturally explains the large energy neutron emission observed in both gallium isotopes. The good agreement with the data indicates that our model includes the relevant configuration spaces.

We tested the applicability of our model by calculating the decay lifetimes and neutron branching ratios for

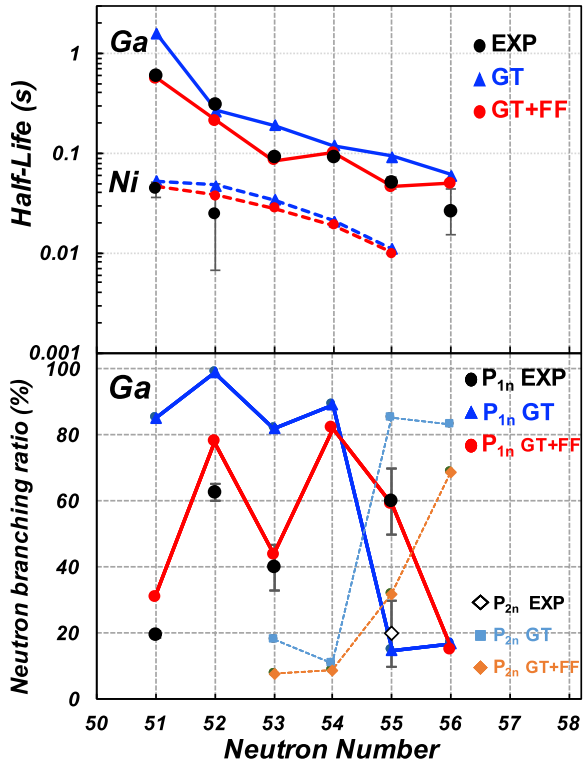

FIG. 3. (Top) Half-life predictions for $N > 50$ gallium (solid line) and nickel (dashed line) isotopes. (Bottom) One (P_{1n}, solid line) and two (P_{2n}, dashed line) β-delayed neutron branching ratio predictions for gallium isotopes. For both panels GT-only predictions are blue diamonds, GT + FF predictions are red circles, and the data are black. Experimental values were taken from [29,30,45,47].

$51 < N < 56$ gallium isotopes. Figure 3 displays the experimental β-decay half-lives (upper panel) and neutron branching ratios (lower panel) compared to calculations including only GT strength (blue stars) and calculations with both GT and forbidden strength included (red circles). In all cases, the forbidden strength was either directly taken or extrapolated from experimental values. The two neutron emission probabilities were determined using a schematic model that did not take into account the partial decay width to one neutron emission. Excluding this effect is known to overestimate the two-neutron emission rate [45,46].

Finally, we employed the same model to estimate the lifetimes of very exotic, $N > 51$, nickel isotopes and compared them with the recent measurements at RIKEN RIBF [47] (top panel of Fig. 3). Here, we followed the same "empirical" procedure where the forbidden strength was extrapolated from the better-known ^{84}Ga data [30]. The error bars correspond to a 500-keV uncertainty in the currently unknown Q_β values. The calculated half-lives and neutron emission probabilities match well the experimental values for both gallium and nickel isotopes.

In conclusion, we observed for the first time high-intensity, high-energy β-delayed neutron emission in ^{83,84}Ga. The large decay strength associated with these transitions indicates that they are allowed Gamow-Teller transformations. Because of the nature of the orbitals above the $N = 50$ gap, GT transitions must involve the decay of neutrons associated with orbitals in the $N = 50$ ^{78}Ni core. A shell model approach capable of dealing with such cross-shell transformations was developed, and its predictions are in excellent agreement with the experimental data. Our model also reproduces the decay lifetimes and delayed neutron branching ratios calculated for the most exotic observed isotopes of gallium and nickel. In particular, the presence of large GT strength at high excitation energies favors high-energy neutron emission and two-neutron emission. Such a large two-neutron branching ratio was recently observed in ^{86}Ga [45]. Large GT strength at high excitation energy resulting in high-energy delayed neutron emission and large two-neutron emission probabilities might be typical for most exotic neutron-rich nuclei, in particular, those along the r-process path of nucleosynthesis.

We thank the HRIBF operations staff for providing the excellent quality radioactive ion beams necessary for this work. This material is based upon work supported by the U.S. Department of Energy (DOE), Office of Science, Office of Nuclear Physics and this research used resources of the Holifield Radioactive Ion Beam Facility of Oak Ridge National Laboratory, which was a DOE Office of Science User Facility. This research was sponsored in part by the National Nuclear Security Administration under the Stewardship Science Academic Alliances program through DOE Award No. DE-FG52-08NA28552. This research was also sponsored by the Office of Nuclear Physics, U.S. Department of Energy under Awards No. DE-AC05-00OR22725 (ORNL), No. DE-FG02-96ER40983 (UTK), and No. DE-FG-05-88ER40407 (VU) and the National Science Foundation.

[1] R. B. Robert, R. C. Meyer, and P. Wang, Phys. Rev. **55**, 510 (1939).
[2] S. M. Bowman, Nuclear Technology **174**, 126 (2011).
[3] M. R. Mumpower, R. Surman, G. C. McLaughlin, and A. Aprahamian, Prog. Part. Nucl. Phys. **86**, 86 (2016).
[4] S. Shalev and G. Rudstam, Phys. Rev. Lett. **28**, 687 (1972).
[5] R. C. Greenwood and A. J. Caffrey, Nucl. Sci. Eng. **91**, 305 (1985).
[6] H. Franz, J.-V. Kratz, K.-L. Kratz, W. Rudolph, G. Herrmann, F. M. Nuh, S. G. Prussin, and A. A. Shihab-Eldin, Phys. Rev. Lett. **33**, 859 (1974).
[7] J. C. Hardy, B. Jonson, and P. G. Hansen, Nucl. Phys. **A305**, 15 (1978).
[8] R. B. Firestone, Phys. Lett. **113B**, 129 (1982).
[9] Y. Fujita, B. Rubio, and W. Gelletly, Prog. Part. Nucl. Phys. **66**, 549 (2011).
[10] P. Moller, B. Pfeiffer, and K.-L. Kratz, Phys. Rev. C **67**, 055802 (2003).
[11] I. N. Borzov, Phys. Rev. C **67**, 025802 (2003).

[12] D.-L. Fang, B. A. Brown, and T. Suzuki, Phys. Rev. C **88**, 034304 (2013).
[13] P. Sarriguren, Phys. Rev. C **91**, 044304 (2015).
[14] D. Martin, A. Arcones, W. Nazarewicz, and E. Olsen, Phys. Rev. Lett. **116**, 121101 (2016).
[15] E. Margaret Burbidge, G. R. Burbidge, W. A. Fowler, and F. Hoyle, Rev. Mod. Phys. **29**, 547 (1957).
[16] H. Nakata, T. Tachibana, and M. Yamada, Nucl. Phys. **A625**, 521 (1997).
[17] M. Madurga *et al.*, Phys. Rev. Lett. **109**, 112501 (2012).
[18] H. W. Schopper, *Weak Interactions and Nuclear Beta Decay* (North-Holland, Amsterdam, 1966).
[19] M. Wang, G. Audi, A. H. Wapstra, F. G. Kondev, M. MacCormick, X. Xu, and B. Pfeiffer, Chin. Phys. C **36**, 1603 (2012).
[20] J. A. Winger *et al.*, Phys. Rev. Lett. **102**, 142502 (2009).
[21] J. A. Winger *et al.*, Phys. Rev. C **81**, 044303 (2010).
[22] J. R. Beene, D. W. Bardayan, A. G. Uribarri, C. J. Gross, K. L. Jones, J. F. Liang, W. Nazarewicz, D. W. Stracener, B. A. Tatum, and R. L. Varner, J. Phys. G **38**, 024002 (2011).
[23] C. J. Gross *et al.*, Nucl. Instrum. Methods Phys. Res., Sect. A **450**, 12 (2000).
[24] W. A. Peters *et al.* (to be published).
[25] S. V. Paulauskas, M. Madurga, R. Grzywacz, D. Miller, S. Padgett, and H. Tan, Nucl. Instrum. Methods Phys. Res., Sect. A **737**, 22 (2014).
[26] S. V. Paulauskas, M. Madurga, R. Grzywacz, and W. A. Peters (to be published).
[27] G. Rudstam and S. Shalev, Nucl. Phys. **A235**, 397 (1974).
[28] K.-L. Kratz *et al.*, Nucl. Phys. **A317**, 335 (1979).
[29] M. F. Alshudifat *et al.*, Phys. Rev. C **93**, 044325 (2016).
[30] K. Kolos *et al.*, Phys. Rev. C **88**, 047301 (2013).
[31] K. W. Scheller, J. Görres, J. G. Ross, M. Wiescher, R. Harkewicz, D. J. Morrissey, B. M. Sherrill, M. Steiner, N. A. Orr, and J. A. Winger, Phys. Rev. C **49**, 46 (1994).
[32] H. Miyatake *et al.*, Phys. Rev. C **67**, 014306 (2003).
[33] Z. Y. Xu, Ph.D. thesis, University of Tokyo, 2014.
[34] D. Testov, Ph.D. thesis, Université Paris Sud, 2014.
[35] B. A. Brown and W. D. M. Rae, Nucl. Data Sheets **120**, 115 (2014).
[36] M. Hjorth-Jensen, T. T. S. Kuo, and E. Osnes, Phys. Rep. **261**, 125 (1995).
[37] B. Cheal *et al.*, Phys. Rev. Lett. **104**, 252502 (2010).
[38] B. Cheal *et al.*, J. Phys. Conf. Ser. **381**, 012071 (2012).
[39] J. S. Thomas *et al.*, Phys. Rev. C **71**, 021302 (2005).
[40] S. Padgett *et al.*, Phys. Rev. C **82**, 064314 (2010).
[41] H. Grawe, in *The Euroschool Lectures on Physics with Exotic Beams*, edited by J. Al-Khalili and E. Roeckl (Springer, Berlin, 2004), Vol I.
[42] P. Moller, W. D. Myers, H. Sagawa, and S. Yoshida, Phys. Rev. Lett. **108**, 052501 (2012).
[43] C. Mazzocchi *et al.*, Phys. Rev. C **92**, 054317 (2015).
[44] E. Caurier, G. Martinez-Pinedo, F. Nowacki, A. Poves, and A. P. Zucker, Rev. Mod. Phys. **77**, 427 (2005).
[45] K. Miernik *et al.*, Phys. Rev. Lett. **111**, 132502 (2013).
[46] T. Kawano, P. Talou, I. Stetcu, and M. B. Chadwick, Nucl. Phys. **A913**, 51 (2013).
[47] Z. Y. Xu *et al.*, Phys. Rev. Lett. **113**, 032505 (2014).